G. Medic
e-mail: gmedic@stanford.edu

P. A. Durbin
e-mail: durbin@vk.stanford.edu

Mechanical Engineering Department,
Stanford University,
Stanford, CA 94305-3030

Toward Improved Prediction of Heat Transfer on Turbine Blades

Reynolds averaged computations of turbulent flow in a transonic turbine passage are presented to illustrate a manner in which widely used turbulence models sometimes provide poor heat transfer predictions. It is shown that simple, physically and mathematically based constraints can substantially improve those predictions. [DOI: 10.1115/1.1458020]

1 Introduction

Three-dimensional numerical simulation of turbulent convective heat transfer is becoming a part of the complex procedure of gas turbine blade design and is slowly replacing simpler two-dimensional methods, mainly based on boundary layer computations and relying heavily on large experimental databases. However, many fundamental and practical developments are needed before full three-dimensional computational analysis becomes reliable.

In the present paper we discuss the effect of anomalous turbulent kinetic energy (k) production on predictions of two-equation turbulence closure models. This problem is known in the literature [1]; the term "stagnation point anomaly" has been used [2,3]. That terminology certainly does not do full justice to this fault. It seems that when a moderate level of turbulent energy is subjected to large rates of strain these models predict exorbitant growth of that energy. It is the large rate of strain, not the stagnation point, that is relevant. The strains occurring in the middle of a turbine passage are sufficient to cause the problem, as will be illustrated herein.

Two explicit proposals to cure the anomalous predicted levels of k are the methods of [4] and [2]. We will assess the ability of these cures to improve heat transfer predictions in turbomachinery flows. Both methods appear quite facile—they can be implemented by a few lines of computer code; but, we will demonstrate that the improvement to predictive accuracy can be quite substantial. Because of their role, these methods are sometimes called "limiters," which is a term that will be used herein.

We have conducted a numerical study of an experimentally documented test case of [5–7] in order to assess different turbulence models. The present paper concerns the flow without film cooling, a companion paper addresses their film-cooling cases. Here the objective is to confirm the value of the limiters, applied to standard eddy-viscosity based turbulence models. This is done by comparison to measurements on the uncooled blade.

2 Turbulence Models and Numerics

In this analysis we are dealing with transonic compressible flow through a gas turbine blade cascade. The equations used to describe the flow are the Favre averaged, compressible Navier-Stokes equations with turbulence models that provide eddy viscosities. The effects of turbulence are taken into account through the constitutive model

$$\mathbf{R} = -\tfrac{2}{3}\rho k I + \mu_t[(\nabla U + \nabla U^T) - \tfrac{2}{3}(\nabla \cdot U)I]$$

$$\dot{\mathbf{q}}_t = -\frac{\mu_t C_p}{\mathrm{Pr}_t}\nabla T \tag{1}$$

for the Reynolds stress and heat flux tensors. To predict the eddy viscosity μ_t the two-layer $k-\varepsilon$, the standard $k-\omega$ and the v^2-f models will be used (see Appendix). The heat flux was computed with a turbulent Prandtl number $\mathrm{Pr}_t = 0.9$.

2.1 Fixes for Anomalous Turbulent Energy. Excessive levels of turbulent kinetic energy are predicted by standard two-equation models in regions of large rate of strain. This was originally recognized in stagnation point flows [4], but it will be seen here that it is a more widespread anomaly. The following reviews two ideas to solve this problem.

Modification of Production. To understand the Kato and Launder [4] approach, consider the closed transport equation for turbulent kinetic energy

$$\partial_t(\rho k) + \nabla\cdot(\rho U k) = \rho P_k - \rho\varepsilon + \nabla\cdot((\mu+\mu_t)\nabla k) \tag{2}$$

where the rate of energy production is given by

$$\rho P_k = R:\nabla U = -\tfrac{2}{3}\rho k(\nabla\cdot U) + 2\mu_t|S|^2 - \tfrac{2}{3}\mu_t(\nabla\cdot U)^2 \tag{3}$$

where $|S|^2 = S_{ij}S_{ji}$ with $S_{ij} = 1/2(\partial_j U_i + \partial_i U_j)$. In nondivergent flow $P_k = 2\nu_t|S|^2$. If one attributes excessive level of k to an over estimate of P_k, then one might look to modifying this term. As a pragmatic device to avoid the problem of spurious stagnation point build-up of turbulent kinetic energy, [4] replaced $|S|^2$ with $|S||\Omega|$ in (3). Here $\Omega_{ij} = 1/2(\partial_j U_i - \partial_i U_j)$ is the vorticity tensor and $|\Omega|$ is its magnitude.

This approach equates the rate of production to zero in irrotational flow ($|\Omega| = 0$); that eliminates the stagnation point problem, because the stagnation point flow is irrotational. While it is not correct that production vanishes in irrotational flow, it might be argued that for applications like heat transfer, the main interest is turbulence produced in the rotational boundary layer. Then little harm is done in replacing $|S|^2$ by $|S||\Omega|$. Difficulties could arise in rotating or swirling flows, where the dependence on $|\Omega|$ might incorrectly increase energy production.

A formal difficulty with setting $P_k = 2\nu_t|S||\Omega|$ is that P_k actually represents transfer of energy from the mean flow to turbulence. Therefore, it should be equal and opposite to a corresponding term in the mean flow energy equation. The term that derives from (1) is $2\nu_t|S|^2$; in other words, the Kato-Launder approach formally violates energy conservation.

Time-Scale Bound. Other perspectives on prediction of excessive levels of turbulent energy are easy to conceive: it could be due to underestimation of dissipation ε, or to over estimation of ν_t. A number of such ideas are subsumed by the idea of a time-scale bound, proposed in [2].

The eddy viscosity predicted by scalar equation turbulence models can be characterized by the form

$$\mu_t = C_\mu \rho u^2 T \tag{4}$$

where u^2 is the velocity scale and T is the turbulence time-scale. In $k-\varepsilon$ and $k-\omega$ models, $u^2 = k$ and in v^2-f model $u^2 = \overline{v^2}$. T equals k/ε, in $k-\varepsilon$ or v^2-f, and it equals $1/(C_\mu\omega)$ in $k-\omega$ [8].

Contributed by the International Gas Turbine Institute for publication in the JOURNAL OF TURBOMACHINERY. Manuscript received by the IGTI, March 20, 2001; revised manuscript received October 15, 2001. Associate Editor: R. Bunker.

T also appears in the source term $(C_{\varepsilon 1}\rho P_k - C_{\varepsilon 2}\rho\varepsilon)/T$ of the ε-equation. Also, production of turbulent energy can be stated as $P_k = C_\mu k|S|^2 T$.

A bound for the turbulent time scale T was derived in [2] from the condition that the eigenvalues of the Reynolds stress tensor in Eq. (1) should be non-negative—which is a sort of "realizability" constraint. The resulting inequality was expressed as a limit on the time-scale

$$T = \min\left[\frac{k}{\varepsilon}, \frac{\alpha}{\sqrt{6}C_\mu|S|}\right]$$

or

$$T = \min\left[\frac{1}{C_\mu\omega}, \frac{\alpha}{\sqrt{6}C_\mu|S|}\right] \tag{5}$$

For compressible flows S should be replaced by $S^* = S - 1/3(\nabla \cdot U)I$. A consequence of (5) is that P_k grows like $|S|$, rather than $|S|^2$ at large rates of strain; this is the theoretical behavior predicted by rapid distortion analysis (see [9]). The value of the coefficient α was selected as $\alpha = 0.6$ in [3] for the v^2-f model. The same value has been applied here to $k-\varepsilon$.

When this technique is invoked with the two-layer formulation, the limiter is applied only in the high Reynolds region. Near the wall the standard $k-l$ formulation, with prescribed l, is applied; the absence of a predictive equation for l obviates the need for a time-scale bound.

2.2 Numerical Method. For numerical solution of the flow equations, we have employed a commercial software package, STAR-CD. STAR-CD is an implicit finite volume solver that employs a variant of the well known SIMPLE method [10], with the turbulence model equations decoupled and solved sequentially. It can be used as a general-purpose convection-diffusion equation solver via user defined subroutines.

Particular turbulence models were programmed through these user defined subroutines. The complete $k-\omega$ and v^2-f models were programmed, while the built-in two-layer $k-\varepsilon$ model was used, with only the time-scale bound coded by a user routine; or in the case of Kato-Launder approach, the modified production term P_k. The bound (5) is usually considered part of the v^2-f formulation.

3 Assessment of Turbulence Models

The test case considered in this analysis is the VKI experiment by [5]. This represents a film-cooled gas turbine rotor blade: the present paper considers their data without film cooling; a companion paper addresses the cooled blade.

The blade chord length, c, equals 80 mm, with pitch-to-chord ratio equal to 0.67, and stagger angle of 38.5 deg. The flow through the cascade is transonic with the inflow conditions: $M_{in} = 0.25$, $Re_{c,in} = 8.5 \cdot 10^5$, $T_{0\infty} = 409.5$ K, and the exit Mach number $M_{ex,is} = 0.92$. The inflow angle is 30 deg and the wall temperature is $T_w = 298$ K. The geometry of the blade is described in more detail in [5].

The inflow turbulence intensity is $Tu_{in} = 5\%$, and the length scale $C_\mu^{3/4}k^{3/2}/\varepsilon$ was estimated as ≈ 1 cm. The presence of ambient turbulence at the entrance to the cascade is pertinent to the problem of the stagnation point anomaly; were Tu set to zero the anomaly would not be noticeable in the heat transfer predictions; but ambient turbulence is a fact of life in turbomachines.

3.1 Heat Transfer Coefficient. The following concentrates on the results that concern blade heat transfer: the surface isentropic Mach number, M_{is}; and the heat transfer coefficient, $h_t = \dot{q}_w/(T_{0\infty} - T_w)$. These quantities are presented with respect to curvilinear coordinate s (normalized by the blade chord c) with the origin at the stagnation point.

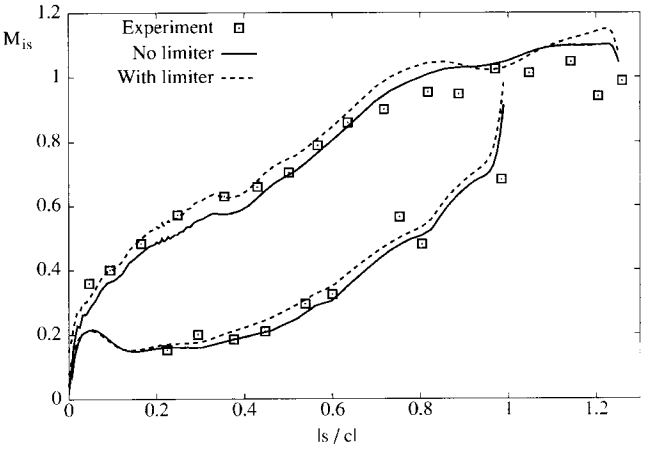

Fig. 1 Isentropic Mach number, M_{is}

The surface pressure distribution is not strongly affected by the choice of turbulence model; to avoid clutter, Fig. 1 only shows computations with $k-\varepsilon$. All the results obtained with limiters virtually coincide with the curve shown. Results obtained with the native $k-\varepsilon$ and $k-\omega$ models, without any limiters, are also almost coincident; they are slightly lower than the results with limiters. This might be understood by attributing the excessive k (or ν_t) levels produced by the native model with greater loss of mean flow energy.

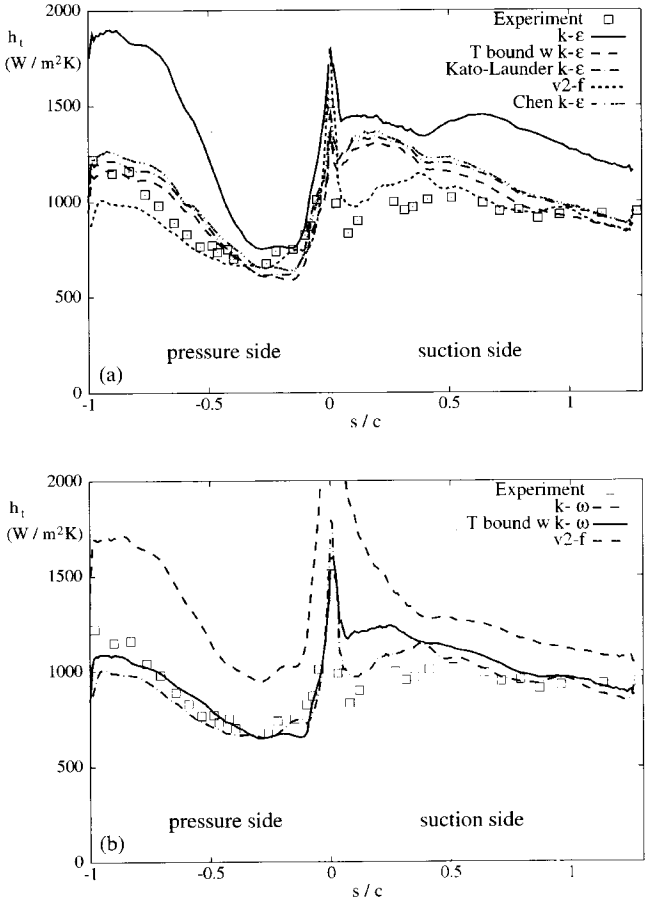

Fig. 2 Heat transfer coefficient h_t (W/m² K)—(*a*) $k-\varepsilon$ models, (*b*) $k-\omega$ models

However, significant differences among the various models are observed when comparing the surface heat transfer coefficients, h_t. These are presented in Fig. 2. The native $k-\varepsilon$ and $k-\omega$ models strongly overpredict the heat transfer coefficient. With either the Kato-Launder formulation, or the bound (5) on the turbulent time-scale, the level of heat transfer is reduced and seems to be predicted more correctly. Obviously, a vast improvement to the performance of $k-\varepsilon$ for some turbomachinery problems can be had quite simply.

Still, there are some discrepancies with the experimental data on the suction side, close to the leading edge of the blade, in the region $0<s/c<0.4$. This region might be a buffeted laminar flow, with transition to turbulence occurring within the region. The substantial overprediction of h_t might be caused partly by failure of the model to capture such processes. The two-layer formulation uses a turbulent length scale next to the wall; hence, it inherently cannot represent transitional regions. But the experimental data seem to imply that, at most, transition might have an influence for $s/c<0.1$—connections to transitional effects are mostly suggestive. Indeed, [5] note that their data for $s/c<0.2$ might have been affected by the film cooling holes, even though they were blocked off during these measurements. It will be shown below that both the limiters clean up the excessive levels of k, so the poor predictions near front of the suction surface are not a residue of the stagnation point anomaly either.

Figure 2 also includes a calculation with the Chen modification to $k-\varepsilon$, as defined in [10]. The same modification is discussed in [11], with the following rationale: the production term in the ε-equation is a dimensionally consistent analogy to that in the k-equation. This could be represented as $P_\varepsilon = F(P_k/\varepsilon)P_k/T$, for an arbitrary function F. The standard model is to make F constant: $F(P_k/\varepsilon)=C_{\varepsilon_1}$. Including the next term in a Taylor series makes F linear: $F(P_k/\varepsilon)=C_{\varepsilon_1}+C_{\varepsilon_3}P_k/\varepsilon$. A small value of $C_{\varepsilon_3}=0.25$ was selected by Chen and C_{ε_1} was reduced to 1.15 to avoid excessive levels of dissipation. The Chen model computation included in Fig. 2 has levels of k in the turbine passage that are similar to those obtained with the methods discussed in Section 2.1 (see Section 3.2).

Prakash [1] first noted that the Chen modification had the potential to prevent excessive growth of k, by increasing ε. He presented computations demonstrating its efficacy. Prakash also recommended clipping the linear term via $C_{\varepsilon_3}\min[3,P_k/\varepsilon]$. (A model that similarly boosts P_ε in highly strained flows is the RNG $k-\varepsilon$ model [10], but excessive levels of k were still seen with that model.)

Finally, the v^2-f model gives results which agree better with the suction side data. Overall, the qualitative distribution of h_t over the suction side looks better with this model. In other studies it has been found that this model produces a reasonable transition location (under zero pressure gradient); again, that property has some suggestive relevance to the improvement in the h_t predictions on the first half of the suction side. Nevertheless, a detailed examination of computed k fields did not show the existence of a transitional zone. Turbulent levels of k were seen in this region, similar to levels obtained with the other models.

Although the v^2-f predictions are much better than those by $k-\varepsilon$ on the *suction side*, it fails to recover to the right heat transfer level near the *pressure side* trailing edge, $s/c<-0.8$. It was suspected that this model might be tending toward relaminarization prematurely; a strongly accelerating pressure gradient can be seen in the lower curve of Fig. 1, beginning around $|s/c|=0.8$. However, here again, a close examination of the turbulent energy field did not confirm this hypothesis.

All models predict a sharp rise of h_t at the stagnation point ($s=0$). Experimental data show a similar behavior. The present geometry is not conducive to assessment of stagnation point heat transfer *per se*. The study by [3] focuses on the need for limiters in stagnation point heat transfer prediction.

Results with $k-\omega$ are similar, altogether, to those obtained with $k-\varepsilon$ model (Fig. 2). Introduction of the bound (5) on the turbulent time scale leads to a significant improvement. Mostly, results lie in between $k-\varepsilon$ and v^2-f.

3.2 Turbulent Kinetic Energy. The reason for the differences in heat transfer prediction obtained with different models must be related to the quantity which links turbulence equations to the mean flow and temperature—the turbulent eddy viscosity. For the present models eddy viscosity is related to the turbulent energy. In order to understand the improvement in heat transfer prediction we consider this quantity. Unfortunately, data for k are not available in the present transonic passage flow.

Examining the values of turbulent kinetic energy predicted in the center of the passage, shows that switching from standard $k-\varepsilon$ (or $k-\omega$) to one of the limiters, or to the v^2-f model, reduces k by a factor on the order of 30 times. This is illustrated in Figs. 3–8 by plotting the turbulent intensity $\mathrm{Tu}=\sqrt{2/3k}/|U|$ field.

The maximum value of intensity in the center of the passage goes from 23 percent, predicted with $k-\varepsilon$ model, to ~3.5 percent predicted with all other models. In other words, all the models except the native $k-\varepsilon$ and $k-\omega$ models predict a decrease of turbulence intensity relative to the inflow value of 5 percent; the latter predict a substantial increase.

The spatial distribution of intensity also differs. Because of the

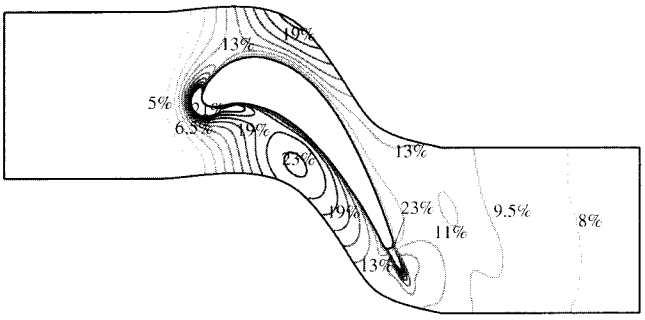

Fig. 3 Turbulence intensity, $k-\varepsilon$ model

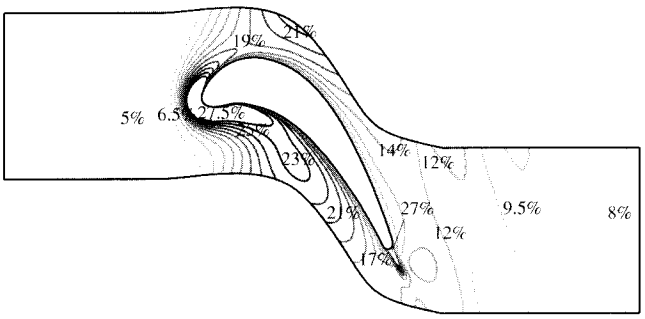

Fig. 4 Turbulence intensity, $k-\omega$ model

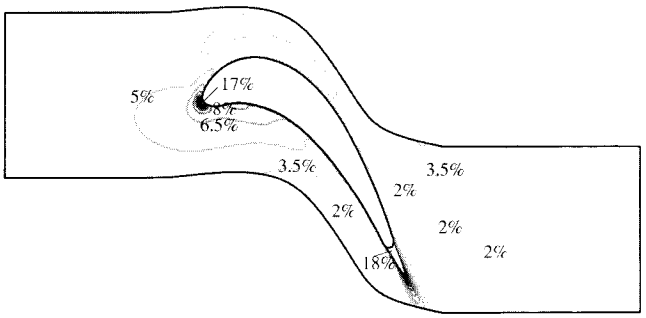

Fig. 5 Turbulence intensity, Kato-Launder $k-\varepsilon$ model

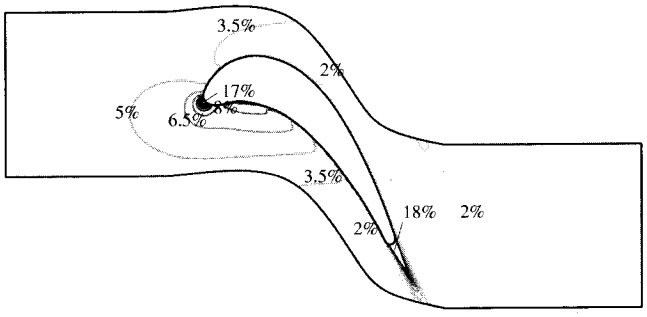

Fig. 6 Turbulence intensity, T bound with $k-\varepsilon$ model

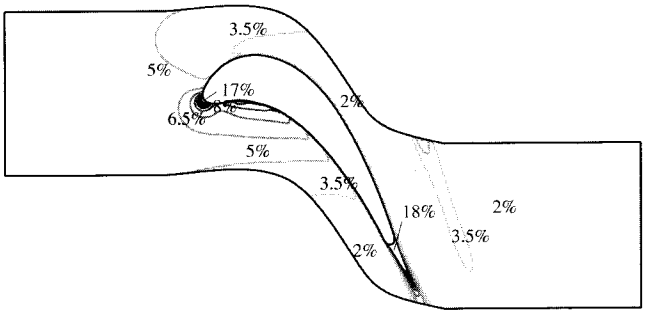

Fig. 7 Turbulence intensity, T bound with $k-\omega$ model

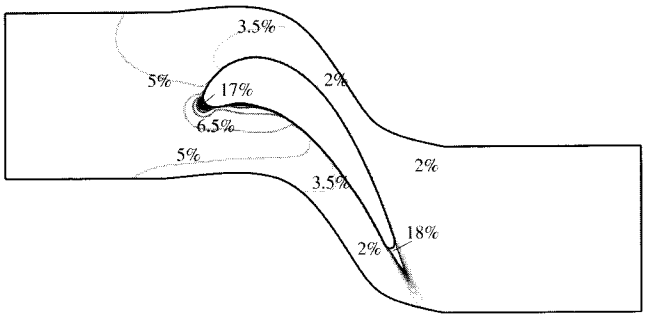

Fig. 8 Turbulence intensity, v^2-f model

normalization by $|U|$, Tu is high at the stagnation point and in the near wake in all of the figures. However, without limiters $k-\varepsilon$ and $k-\omega$ predict a pocket of high intensity below the pressure surface, while the other models show a monotonic decline of Tu through the passage. The bulge in the profile of h_l shown by the upper curve in Fig. 2 is not surprising in light of Fig. 3. That effect seems to be even more important in the case of $k-\omega$ model, which gives a peak value of 27.5 percent in the stagnation point region.

It might at first seem odd that the intensity *drops* in the strongly accelerating flow through the cascade passage. Indeed the turbulent energy rises from 37.5 to a maximum of 80 m^2/s^2 (in v^2-f computations, for instance), but the mean flow velocity increases more than $\sqrt{k}$, so that their ratio actually decreases. This behavior is qualitatively consistent with experiments in [12] and [13], and is also predicted by rapid distortion theory [9]. By contrast, $k-\varepsilon$ and $k-\omega$ with no limiters predict such an excessive increase of k that the turbulent intensity actually *increases*. The theory and limited data, just cited, argue strongly that this is unphysical.

In order to locate the regions where the standard $k-\varepsilon$ model violates the bound on the turbulent time scale, Figs. 9 and 10 present the ratio $T/T_{\lim}$, where $T=k/\varepsilon$ and $T_{\lim}=1/(\sqrt{6}C_\mu|S|)$. This ratio is plotted for two different values of the inflow turbulent dissipation rate ε. Where the ratio is greater than unity the limiter comes into play.

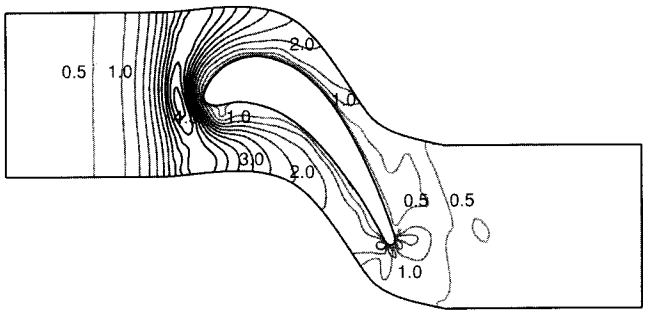

Fig. 9 $T/T_{\lim}$, $k-\varepsilon$ model, lower inflow value of ε, $l_\varepsilon = C_\mu^{3/4}k^{3/2}/\varepsilon = 0.01$ m

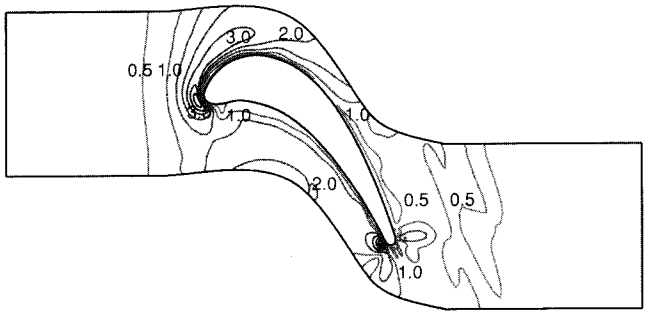

Fig. 10 $T/T_{\lim}$ $k-\varepsilon$ model, higher inflow value of ϵ, $l_\epsilon = C_\mu^{3/4}k^{3/2}/\epsilon = 0.001$ m model is used in any particular application

A higher level of inlet dissipation was used in Fig. 10. Such a device might be considered as an alternative method to reduce turbulent energy—cause it to decay before it reaches the blade. We consider this only because it has sometimes been noted that predictions can be improved by tuning the inlet conditions. While setting a higher value of inflow ε certainly does reduce the region where the time-scale inequality is violated, the stagnation point build-up of turbulent kinetic energy still presents a problem. Furthermore, increasing the inflow dissipation rate ε may lead to too strong decay of inflow turbulence, and therefore to the generation of flow conditions which differ from the actual situation of interest. With the limiter in place the model becomes much less sensitive to the inlet l_ε, since there is then no anomaly, even when l_ε is large.

In that sense, inclusion of the bound on turbulent time scale in the $k-\varepsilon$, or $k-\omega$, model represents a way to automatically preempt possible spurious predictions. Adjusting the inflow turbulence dissipation rate ε is not a generally applicable fix.

4 Conclusion

With the time-scale bound in place, rather good predictions are obtained using the two layer $k-\varepsilon$ model. This suggests that some of the failures reported in the literature may result from anomalous k production; an anomaly for which rather simple cures have been proposed.

We have shown herein that substantially improved heat transfer predictions can indeed be obtained by invoking these limiters. It should be emphasized that without the limiters, the excessive levels in the turbine passage are so high that they are actually the origin of over predictions of h_l—high levels of k near the stagnation point are not the only culprit.

Our objective in this paper has been to draw attention to an improvement that can be made to widely used turbulence models. Other considerations might determine which model is used in any particular application.

Appendix

Two-Layer Formulation of $k-\varepsilon$ Model. The two-layer method consists in patching together the $k-l$ and $k-\varepsilon$ models. The standard model equation for turbulent kinetic energy is

$$\partial_t(\rho k)+\nabla\cdot(\rho U k)=\rho P_k-\rho\varepsilon+\nabla\cdot((\mu+\mu_t)\nabla k) \tag{6}$$

where

$$\rho P_k=R:\nabla U=-\tfrac{2}{3}\rho k(\nabla\cdot U)+2\mu_t|S|^2-\tfrac{2}{3}\mu_t(\nabla\cdot U)^2 \tag{7}$$

with $S_{ij}=1/2(\partial_j U_i+\partial_i U_j)$ and μ_t being the eddy viscosity. It is used in both the $k-l$ and $k-\varepsilon$ formulations.

In the $k-\varepsilon$ model, Eq. (6) is supplemented by

$$\partial_t(\rho\varepsilon)+\nabla\cdot(\rho U\varepsilon)=\frac{C_{\varepsilon 1}\rho P_k-C_{\varepsilon 2}\rho\varepsilon}{T}+\nabla\cdot\left(\left(\mu+\frac{\mu_t}{\sigma_\varepsilon}\right)\nabla\varepsilon\right) \tag{8}$$

where the turbulence time-scale is $T=k/\varepsilon$ and the eddy viscosity is

$$\mu_t=C_\mu\rho kT \tag{9}$$

The standard model constants are

$$C_{\varepsilon 1}=1.44;\quad C_{\varepsilon 2}=1.92;\quad \sigma_\varepsilon=1.3;\quad C_\mu=0.09$$

In the $k-l$ model, the dissipation rate is represented by

$$\varepsilon=\frac{k^{3/2}}{l_\varepsilon} \tag{10}$$

and the eddy viscosity is

$$\mu_t=C_\mu\rho\sqrt{k}l_\nu \tag{11}$$

These supplement the k-equation (6). The VonDriest form for the length scales will be adopted here

$$l_\varepsilon=C_{ly}(1-e^{-R_y/A_\varepsilon});\quad l_\nu=C_l y(1-e^{-R_y/A_\nu}) \tag{12}$$

$R_y=y\rho\sqrt{k}/\mu$ is a wall-distance Reynolds number in which, for smooth walls, y is distance from the wall. The log-layer solution requires that $C_l=\kappa/C_\mu^{3/4}$ where κ is the VonKarman constant. The widely accepted value of $\kappa=0.41$ gives $C_l=2.5$. The requirement that $k\to\varepsilon y^2/2\nu$ as $y\to 0$ gives $A_\varepsilon=2C_l=5.0$. There is only one free constant, A_ν. The value $A_\nu=62.5$ was chosen for use with the two-layer formulation. This number gave very good agreement between C_f versus R_θ predictions and experiments for zero pressure gradient, flat plate boundary layers.

The two-layer formulation consists simply of using (11) and (10) near a wall, and switching abruptly to (9) and (8) at a patching point. The patching point is defined as the location where the damping function $1-e^{-R_y/A_\nu}$ equals 0.95; i.e., where $y=\log(20)A_\nu\nu/\sqrt{k}$. For solid walls, the boundary condition $k(0)=0$ is applied.

$k-\omega$ Model. In Wilcox's original $k-\omega$ model, the eddy viscosity is defined as $\mu_t=C_\mu\rho kT$, with turbulence time-scale $T=1/(C_\mu\omega)$; in other words, $\mu_t=\rho k/\omega$.

The original $k-\omega$ model equation for turbulent kinetic energy is

$$\partial_t(\rho k)+\nabla\cdot(\rho U k)=\rho P_k-C_\mu\rho\omega k+\nabla\cdot((\mu+\sigma_k\mu_t)\nabla k) \tag{13}$$

where

$$\rho P_k=R:\nabla U=-\tfrac{2}{3}\rho k(\nabla\cdot U)+2\mu_t|S|^2-\tfrac{2}{3}\mu_t(\nabla\cdot U)^2 \tag{14}$$

Equation (13) is supplemented by the equation for the specific dissipation rate ω

$$\partial_t(\rho\omega)+\nabla\cdot(\rho U\omega)=\frac{1}{T}\left(\frac{\gamma_1}{C_\mu k}\rho P_k-\frac{\beta_1}{C_\mu}\rho\omega\right)+\nabla\cdot(\mu+\sigma_\omega\mu_t)\nabla_\omega) \tag{15}$$

The original model constants are

$$\sigma_k=0.5;\quad \sigma_\omega=0.5;\quad \gamma_1=5/9;\quad \beta_1=0.075;\quad C_\mu=0.09$$

The boundary conditions for solid walls ($y\to 0$) are

$$k(0)=0,\quad \omega\to\frac{6\nu}{\beta_1 y^2} \tag{16}$$

$\overline{v^2}-f$ Model. The eddy viscosity is now defined as $\mu_t=C_\mu\rho\overline{v^2}T$, with the turbulence time-scale T

$$T=\min\left[\max\left[\frac{k}{\varepsilon},6\sqrt{\frac{\nu}{\varepsilon}}\right],\frac{\alpha k}{\sqrt{6}\,\overline{v^2}C_\mu|S|}\right] \tag{17}$$

with $\alpha=0.6$.

The equations for k and ε, (6) and (8), respectively, are supplemented with the equation for $\overline{v^2}$

$$\partial_t(\rho\overline{v^2})+\nabla\cdot(\rho U\overline{v^2})=\rho kf-\rho N\frac{\overline{v^2}}{k}\varepsilon+\nabla\cdot((\mu+\mu_t)\nabla\overline{v^2}) \tag{18}$$

with f representing the nonlocal effects

$$f-L^2\Delta f=(C_{f1}-1)\frac{2/3-\overline{v^2}/k}{T}+C_{f2}\frac{P_k}{k}+(N-1)\frac{\overline{v^2}}{kT} \tag{19}$$

where the turbulent length scale L is

$$L=C_L\max\left[\min\left[\frac{k^{3/2}}{\varepsilon},\frac{k^{3/2}}{\sqrt{6}\,\overline{v^2}C_\mu|S|}\right],C_\eta\frac{\nu^{3/4}}{\varepsilon^{1/4}}\right] \tag{20}$$

For solid walls, when $y\to 0$, this yields

$$k(0)=0;\quad \overline{v^2}(0)=0,\quad \varepsilon\to\frac{2\nu k}{y^2},\quad f\to-\frac{4(6-N)\nu^2\overline{v^2}}{\varepsilon y^4} \tag{21}$$

The original v^2-f model with $N=1$ was later modified (see [3], [14]) in order to avoid the numerical difficulties due to strong nonlinear coupling of turbulence variables through the boundary conditions (21) and the value of $N=6$ was chosen.

An additional modification was to eliminate the wall distance y from the equation for C_{e1} resulting in the following values of model constants used for the modified model:

$$C_\mu=0.22;\quad C_{\varepsilon 1}=1.4(1+0.050\sqrt{k/\overline{v^2}});\quad C_{\varepsilon 2}=1.9;$$
$$C_{f1}=1.4;\quad C_{f2}=0.3;\quad C_L=0.23;\quad C_\eta=70 \tag{22}$$

In this analysis we used this modified version of v^2-f model.

Acknowledgment

This work was sponsored by General Electric aircraft engines. We are grateful to Drs. Chander Prakash and Gary Steuber for private communications concerning their work at General Electric on excessive k production.

Nomenclature

M = Mach no.
$\mathrm{Re}_{c,\mathrm{in}}$ = inflow Reynolds no. (based on chord length c)
T_o = total temperature
T_w = wall temperature
Tu = turbulence intensity $=\sqrt{2/3k}/|U|$
c = blade chord

h_t = heat transfer coefficient $= \dot{q}_w/(T_{o\infty} - T_w)$
$\dot{q}_w$ = wall heat flux rate
s = curvilinear coordinate

Subscripts

∞ = free stream
in = inflow
ex = exit
w = wall
o = total conditions
is = isentropic conditions

References

[1] Prakash, C., 1995, "Some Experiences With the Standard $k-\varepsilon$, RNG and Chen Turbulence Models," *National Turbulent Combustion Model Meeting, NASA Lewis*, July 27–28.

[2] Durbin, P. A., 1996, "On the $k-\varepsilon$ Stagnation Point Anomaly," Int. J. Heat Fluid Flow, **17**, pp. 89–90.

[3] Behnia, M., Parneix, S., Shabany, Y., and Durbin, P. A., 1999, "Numerical Study of Turbulent Heat Transfer in Confined and Unconfined Impinging Jets," Int. J. Heat Fluid Flow, **20**, pp. 1–9.

[4] Kato, M., and Launder, B. E., 1993, "Modelling Flow-Induced Oscillations in Turbulent Flow Around a Square Cylinder," ASME FED **157**, pp. 189–199.

[5] Camci, C., and Arts, T., 1985, "Short Duration Measurements and Numerical Simulation of Heat Transfer Along the Suction Side of a Film-Cooled Gas Turbine Blade," ASME J. Eng. Power, **107**, pp. 991–997.

[6] Camci, C., and Arts, T., 1985, "Experimental Heat Transfer Investigation Around the Film-Cooled Leading Edge of a High-Pressure Gas Turbine Rotor Blade," ASME J. Eng. Power, **107**, pp. 1016–1021.

[7] Camci, C., and Arts, T., 1990, "An Experimental Convective Heat Transfer Investigation Around a Film-Cooled Gas Turbine Blade," ASME J. Turbomach., **112**, pp. 497–503.

[8] Wilcox, D. C., 1993, *Turbulence Modeling for CFD*, DCW Industries, Inc., La Canada, CA.

[9] Durbin, P. A., and Pettersson Reif, B. A., 2001, *Statistical Theory and Modeling for Turbulent Flow*, John-Wiley & Sons, New York, NY.

[10] *STAR-CD Version 3.10—Methodology, 1999*, Computational Dynamics Limited.

[11] Durbin, P. A., 1990, "Turbulence Modeling Near Rigid Boundaries," *CTR Annual Research Briefs*, Stanford University, Stanford, CA.

[12] Radomsky, R. W., and Thole, K. A., 2000, "Flowfield Measurements for a Highly Turbulent Flow in a Stator Vane Passage," ASME J. Turbomach., **122**, pp. 255–262.

[13] Priddy, W. J., and Bayley, F. J., 1988, "Turbulence Measurements in Turbine Blade Passages and Implications for Heat Transfer," ASME J. Turbomach., **110**, pp. 73–79.

[14] Lien, F. S., and Kalitzin, G., 2001, "Computations of Transonic Flows With the v^2-f Turbulence Model," Int. J. Heat Fluid Flow, **22**, pp. 53–61.